AIP | Applied Physics Letters

Magnetic behavior of graphene sheets embedded carbon film originated from graphene nanocrystallite

Chao Wang and Dongfeng Diao

Citation: Appl. Phys. Lett. **102**, 052402 (2013); doi: 10.1063/1.4790283
View online: http://dx.doi.org/10.1063/1.4790283
View Table of Contents: http://apl.aip.org/resource/1/APPLAB/v102/i5
Published by the American Institute of Physics.

Related Articles

Suppression of low-temperature ferromagnetic phase in ultrathin FeRh films
J. Appl. Phys. 113, 123909 (2013)

The oxygen vacancy effect on the magnetic property of the LaMnO3−δ thin films
Appl. Phys. Lett. 102, 122402 (2013)

Three-dimensional mapping of the anisotropic magnetoresistance in Fe3O4 single crystal thin films
J. Appl. Phys. 113, 17B103 (2013)

Magnetic stability of ultrathin FeRh films
J. Appl. Phys. 113, 17C107 (2013)

The low-frequency alternative-current magnetic susceptibility and electrical properties of Si(100)/Fe40Pd40B20(XÅ)/ZnO(500Å) and Si(100)/ZnO(500Å)/Fe40Pd40B20(YÅ) systems
J. Appl. Phys. 113, 17B303 (2013)

Additional information on Appl. Phys. Lett.

Journal Homepage: http://apl.aip.org/
Journal Information: http://apl.aip.org/about/about_the_journal
Top downloads: http://apl.aip.org/features/most_downloaded
Information for Authors: http://apl.aip.org/authors

ADVERTISEMENT

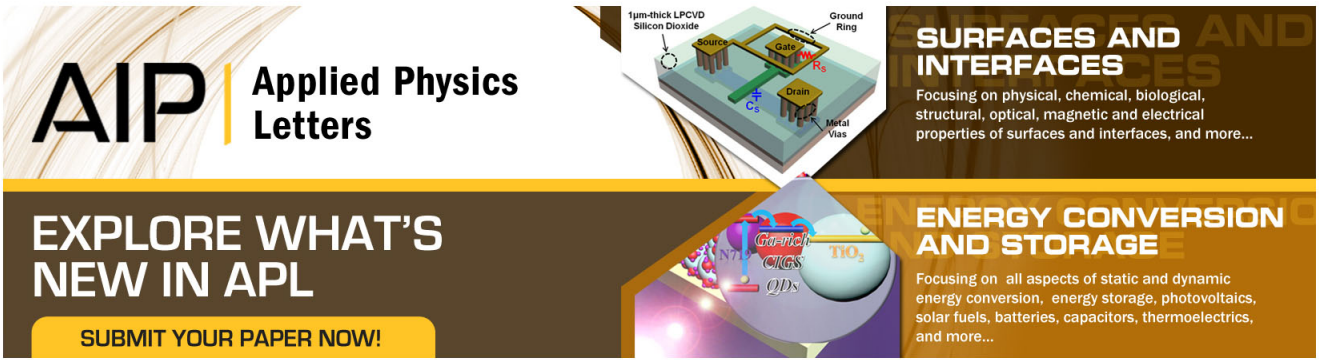

Downloaded 27 Mar 2013 to 117.32.153.158. This article is copyrighted as indicated in the abstract. Reuse of AIP content is subject to the terms at: http://apl.aip.org/about/rights_and_permissions

Magnetic behavior of graphene sheets embedded carbon film originated from graphene nanocrystallite

Chao Wang and Dongfeng Diao[a)]
Nanosurface Science and Engineering Research Institute, College of Mechatronics and Control Engineering, Shenzhen University, Shenzhen 518060, China and Key Laboratory of Education Ministry for Modern Design and Rotor-Bearing System, School of Mechanical Engineering, Xi'an Jiaotong University, 710049 Xi'an, China

(Received 16 July 2012; accepted 21 January 2013; published online 5 February 2013)

We found paramagnetic behavior at 300 K of graphene sheets embedded carbon (GSEC) film, which is deposited under low energy electron irradiation in electron cyclotron resonance plasma. The origin of the magnetic properties of GSEC film is ascribed to the formation of graphene nanocrystallite. With higher irradiation energy, the size of nanocrystallite barely changed, while the density in GSEC film became higher, leading to a dramatically increase of saturation magnetization and residual magnetism. This finding indicates that GSEC film with higher magnetization can be expected, which has the potential for magnetic and spintronics applications. © *2013 American Institute of Physics*. [http://dx.doi.org/10.1063/1.4790283]

The magnetism of carbon nanomaterials has drawn much interest ever since the ferromagnetic C_{60} was reported.[1] Thereafter, magnetic behaviors have been found in other carbon allotropies such as nanofoam[2] and nanofibers.[3] However, these magnetic carbon materials are not suitable for nanodevice application, since their shape and size are usually uncertain due to the preparing method. Meanwhile, although the mechanism was not very clear, one opinion was proposed that the intrinsic magnetism in carbon materials origins from the spin of uncoupled electrons.[2] Based on this fundamental understanding, another kind of approaches was developed, which is to create defects in perfect graphite or diamond structure.[4] For instance, high oriented pyrolytic graphite (HOPG)[5] and nanodiamond[6] were irradiated by ions in order to induced magnetic property. This method made the shape and size of the magnetic carbon material designable. But the procedure was usually complicated and demanding special facilities such as ion sources. Recently, graphene based material became a new path to obtain better magnetic performances, because it shows unique electron structure and mechanical properties for potential utilities in nanomachinery. There were theoretical and experimental studies on magnetic graphene oxide,[7–9] graphene nanoflakes,[10,11] and hydrogenated graphene.[12,13] However, the experimental results are still not satisfying and the procedures are not simple enough. Lately, we have reported our method to directly preparing graphene sheets embedded carbon (GSEC) film by using low energy electron irradiation during deposition.[14] In this study, we further report the paramagnetic behavior of GSEC film at room temperature of 300 K. The origin of its magnetic properties is explained in relationship with the defects at the edges of small size embedded graphene nanocrystallite.

The electron cyclotron resonance (ECR) plasma sputtering system was used for film deposition. The film was prepared using low energy electron irradiation technique, which was developed in our former research.[14] In this study, three irradiation energies of 10, 50, and 100 eV were selected to obtain films with different nanostructures for magnetic behavior study. For comparison, the carbon target material (named pristine carbon) was also studied in the following research. The films were deposited for 1 h with the growth rate of 4 nm per minute.

The film nanostructures were characterized through transmission electron microscope (TEM) with 200 kV acceleration voltage and Raman spectrometer with 514 nm laser excitation. Figure 1 showed the Raman spectra of the pristine carbon and the films prepared with different electron irradiation energy. The spectrum of pristine carbon and 10 eV irradiation sample show a board band from 1100 to 1800 cm^{-1}, representing the amorphous structure. The spectrum of 50 and 100 eV irradiation sample (GSEC films) showed separated *D* and *G* band around 1350 and 1580 cm^{-1}, and a medium strong 2*D* band around 2690 cm^{-1}, which is the feature of graphene structure with less than 5 layers.[15,16] The low-wave-number part between 1100 cm^{-1} and 1800 cm^{-1} is decomposed into a Lorentz shaped *D* band and a Breit-Winger-Fano (BWF) shaped

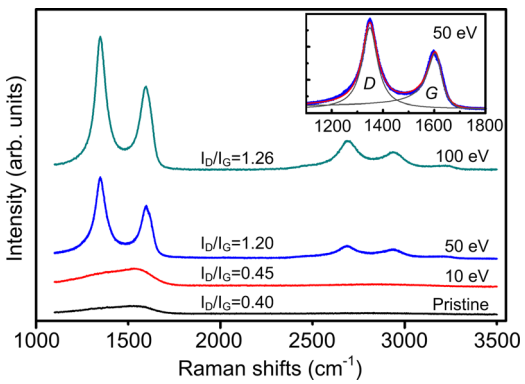

FIG. 1. Raman spectrum of pristine carbon target and carbon films deposited with electron irradiation energy of 10, 50, and 100 eV. The inset figure shows fitting result of 50 eV irradiation sample from 1100 cm^{-1} to 1800 cm^{-1}, including original spectrum (blue), fitting result (red), D band, and G band (grey).

[a)]Author to whom correspondence should be addressed. Electronic mail: dfdiao@mail.xjtu.edu.cn.

 © 2013 American Institute of Physics

Downloaded 27 Mar 2013 to 117.32.153.158. This article is copyrighted as indicated in the abstract. Reuse of AIP content is subject to the terms at: http://apl.aip.org/about/rights_and_permissions

G band.[17] The fitted G band center was right shifted due to the BWF method[18]

$$\omega = \omega_0 - \Gamma/2|Q|, \quad (1)$$

where ω is the actual G band center, ω_0 is the fitted G band center, Γ is the full width at the half maximum (FWHM), and Q is the fitting coefficient. By fitting the D and G bands, the ratios of D band to G band (I_D/I_G) are obtained as 0.40, 0.45, 1.20, 1.26 for pristine carbon, 10, 50, and 100 eV irradiation sample, respectively. From the above fitting results, more quantitative results can be derived. It has been found that the grain size inside carbon film is related to I_D/I_G.[3,17,19–21] To be specific, the in-plane size of graphene sheet grain size (L_α) can be described by the following equations:[20,21]

$$I_D/I_G = C(\lambda)/L_\alpha \ (L_\alpha > 2\text{nm}), \quad (2)$$

$$I_D/I_G = C'(\lambda) \cdot L_\alpha^2 (L_\alpha < 2\text{nm}), \quad (3)$$

where C and C′ are coefficients related to excitation laser wavelength. In our case, $C(\lambda = 514\,\text{nm})$ is 4.362 nm and $C'(\lambda = 514\,\text{nm})$ is 0.55 nm^{-2}, respectively. From the TEM observation,[14] we have recognized the size of graphene nanocrystallite in the GSEC films is 3 to 5 nm, while the pristine carbon target and amorphous carbon film showed non-crystalline structure, which meant their grain sizes were less than 2 nm. So the average in-plane size of graphene sheet in the four samples can be estimated from their I_D/I_G values by introducing Eq. (2) for GSEC film and Eq. (3) for amorphous carbon. Therefore, L_a of the four samples are 0.85, 0.90, 3.64, and 3.46 nm, respectively. It is obvious that the calculated grain sizes of the four samples are in good agreement with the TEM observation. In addition, the similar grain size of the two GSEC films indicates that increasing irradiation energy from 50 eV to 100 eV did not lead to larger graphene nanocrystallite. However, we noticed that the Raman bands intensity of the 100 eV irradiation sample was twice stronger than those of the 50 eV irradiation sample. We believe this is caused by the increasing of nanocrystallite content. The X-ray photoelectron spectroscopy results showed that the sp^2 content increased from 71% to 81% as the irradiation energy increased from 50 eV to 100 eV. This also can be seen as a result of the increasing nanocrystallite content. So the increasing irradiation energy causes more nanocrystallite in the GSEC film, while the grain size remains 3 to 4 nm.

In order to study the magnetic property of GSEC film, the films were scratched off the substrate carefully and collected onto a plastic foil with a diamond-tip-pencil. The foil was then folded and packed into the plastic capsule. Magnetization measurements were carried out with a SQUID MPMS-XL-7 from Quantum Design at the constant temperature of 300 K. The applied magnetic field was from −10 kOe to 10 kOe. Figure 2 shows the measured magnetic moment of 50 eV irradiation GSEC film together with plastic foil (red circle) as well as the plastic foil (black open square). The weights of plastic foil with and without GSEC film are 111.4 mg and 110.4 mg, respectively. Thus, the GSEC film weight is calculated to be 1 mg.

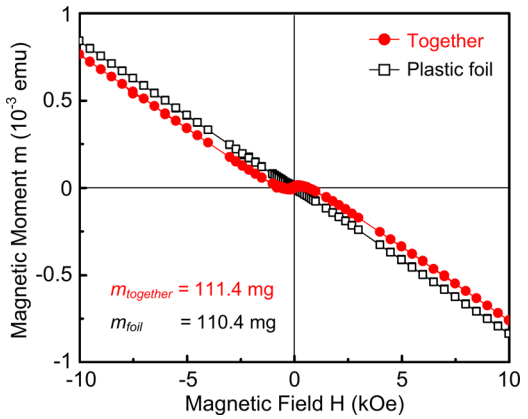

FIG. 2. The total magnetic moment (in units of 10^{-3} emu = 10^{-6} A·m^2) without any background subtraction of the plastic foil together with GSEC film (red circle) and without GSEC film (black open square). The measurement was carried out at T = 300 K as a function of magnetic field (1 kOe = $10^6/4\pi$ A·m^{-1}) by cycling the field from +10 kOe to −10 kOe and back to +10 kOe.

The figure clearly shows an S-shaped curve for GSEC film together with the plastic foil, which suggests a paramagnetic behavior at 300 K. Since the plastic foil is antimagnetic as indicated by the liner curve, we ascribe the paramagnetic behavior to the GSEC film.

The magnetic moment of carbon films was obtained by subtraction of the plastic foil signal and further conversed into unit magnetic moment. The results for pristine carbon, 10, 50, and 100 eV irradiation samples are shown in Figure 3. It is obvious that the pristine carbon has the least saturation magnetization (M_s), and M_s become larger as the irradiation energy increases from 10 to 100 eV. Especially the 100 eV irradiation sample has the M_s of 0.265 emu/g, which is about ten times larger than pristine carbon. From the inset graph, the hysteresis loops of the four samples can be clearly seen. In this graph, the effect of electron irradiation energy on the magnetic behavior of GSEC film is more obvious, where the hysteresis loops of 100 eV irradiation sample looks remarkably large comparing to the other three samples. The residual magnetism (B_r) and coercive force (H_c) also increased dramatically. From the standpoint of application in magnetic record field, these higher B_r and larger H_c are

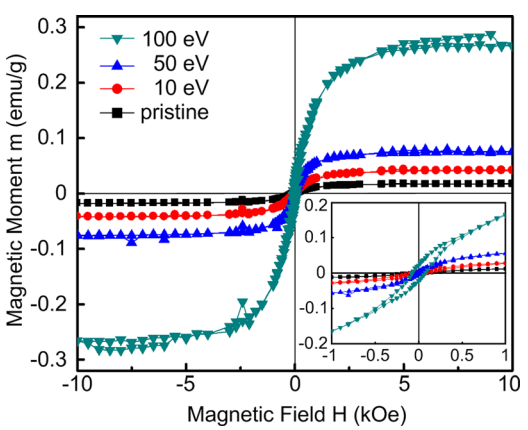

FIG. 3. Unit magnetic moment (emu/g) after subtraction of background magnetic moment for the pristine carbon and carbon film with irradiation energy of 10, 50, and 100 eV. The inset graph shows a smaller field region of the hysteresis loops.

Downloaded 27 Mar 2013 to 117.32.153.158. This article is copyrighted as indicated in the abstract. Reuse of AIP content is subject to the terms at: http://apl.aip.org/about/rights_and_permissions

TABLE I. Magnetization (emu/g) at 300 K of GSEC film and some reported graphene based materials.

Reduced graphene oxide[a]	~0.4 (0.3 T)
Hydrogenated graphene[a]	~0.007 (0.3 T)
Proton irradiated HOPG[b]	~0.02 (1 T)
Annealed graphene oxide[c]	~0.02 (1 T)
GSEC film (50 eV irradiation)	~0.0745 (0.3 T)
GSEC film (100 eV irradiation)	~0.265 (0.3 T)

[a]The magnetization of reduce graphene oxide and hydrogenated graphene, see Ref. 4.
[b]The magnetization of proton irradiated HOPG, see Ref. 5
[c]The magnetization of annealed graphene oxide, see Ref. 8.

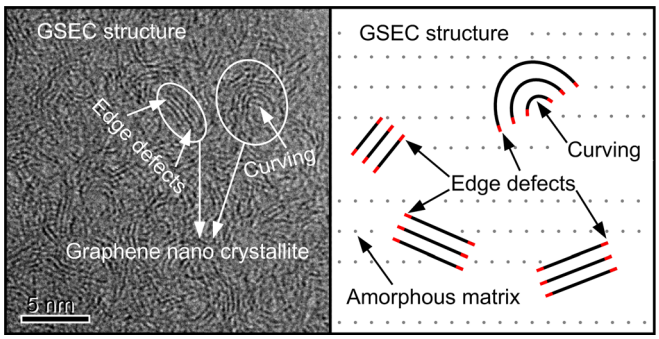

FIG. 4. GSEC structure obtained from TEM observation (left side), in which the edge defects and curving of graphene nanocrystallite are labeled by arrows. For clearer recognition, a schematic image is drawn (right side).

preferred since they can bring about stronger magnetic record ability.

For clearer comparison, Table I exhibits some reported magnetic graphene based materials and their magnetizations at 300 K, a temperature close to real application. Apparently, the magnetization of 100 eV irradiation GSEC film is larger than most of the listed materials. Moreover, all the other materials are either random flakes or films that need heavy ion irradiation, which make them inconvenient for large scale production. On the other hand, GSEC films can be directly deposited in large scale and the three dimensional shapes can be easily controlled. Although the in-plane directions of graphene nanocrystallites are random, their vertical growing direction is normal to the substrate. If the magnetization can be further increased, the GSEC films will be more convenient and economical for magnetic and spintronics applications.

The origin of carbon magnetism has been studied in both theoretical[22–26] and experimental[2,3] manners, and the inner defects were found responsible for the paramagnetic behavior. In theoretical studies, the origin of carbon magnetism was ascribed to either unsaturated graphene edge atoms[22–25] or certain curving of graphene sheet which can produce radicals.[26] In experimental researches, it was found from electron spin resonance results that the dangling sp^2 atoms at the edge and defect positions can provide magnetic moment.[2,3] As long as the edge defects and curving in graphene based structures were considered as the reason for magnetic behavior, these structures have not been clearly found out in a visible approach. In GSEC structure, the edge defects and curving of graphene sheets can be identified clearly in the TEM image, as shown in Figure 4. It can be seen from the figure that the graphene nanocrystallite contains a lot of edge atoms due to their small sizes. The neighboring graphene sheets aligned parallel, which can lead to magnetic moment coupling between edge atoms. The curving of the graphene sheets may also lead to free spin of sp^2 atoms. In fact, we found the magnetization of GSEC structure increases with the increment of nanocrystallite content in the film, which will be described in detail in the following. So the intrinsic magnetic property may be ascribed to the formation of graphene nanocrystallite.

In our research, we noticed that the increasing electron irradiation energy effectively improved the magnetic behavior of GSEC film. As the irradiation energy reached 50 eV, the film structure changes from amorphous to GSEC, and the magnetic properties M_s and B_r increased slightly comparing to the pristine and amorphous state, as shown in Figure 5(a). However, the grain size of the graphene nanocrystallite has dramatically increased from less than 1 nm to 3.46 nm, as shown by the blue curve in Figure 5(b). Moreover, as the irradiation energy increased to 100 eV, the grain size barely changes, while the M_s and B_r notably increased together. This means the grain size has little relationship with the magnetic performances.

On the contrary, when GSEC structure is formed, M_s and B_r increase greatly with sp^2 increment, which is clearly shown by the red curve in Figure 5(b). This can be ascribed to the increasing of graphene nanocrystallite content. Since the graphene sheets contains many defect atoms, which can create magnetic moment through spin arrangement, the increasing of nanocrystallite can lead to stronger magnetization. This result indicates that it is very effective to increase graphene nanocrystallite density in the film rather than grown nanocrystallite with larger size, because the former method can obtain much more edge defects. It is highly possible that if the content of graphene nanocrystallite further increased, the magnetization of GSEC structure could consequently became larger. This is an interesting way to obtain carbon nanostructures with high magnetization, which will be investigated in the following study.

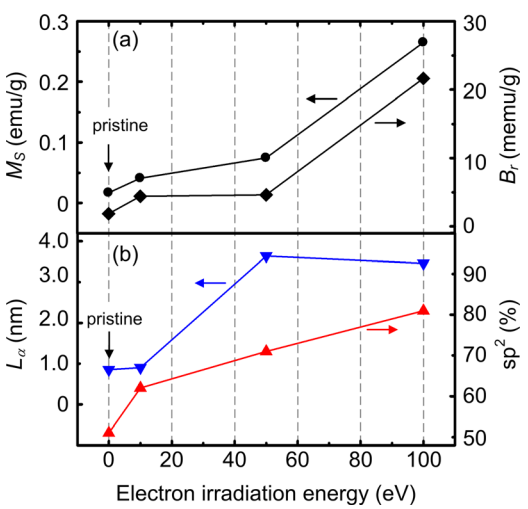

FIG. 5. The (a) saturation magnetization M_s at 300 K, residual magnetism B_r at 300 K, (b) average grain size L_α and sp^2 content of pristine carbon and carbon films with different electron irradiation energy.

Downloaded 27 Mar 2013 to 117.32.153.158. This article is copyrighted as indicated in the abstract. Reuse of AIP content is subject to the terms at: http://apl.aip.org/about/rights_and_permissions

In conclusion, we found paramagnetic behavior at 300 K of GSEC film which was directly obtained by using low energy electron irradiation during deposition. With irradiation energy of 100 eV, the GSEC film has the saturation magnetization of 0.265 emu/g, which is larger than most graphene based materials ever reported. The origin of magnetic property of GSEC film was ascribed to the formation of graphene nanocrystallite. The increasing of irradiation energy lead to higher nanocrystallite density, while the grain size barely changed. An effective method to improve the magnetic properties of GSEC film has been discovered, which is to increase the nanocrystallite density in the film rather than gain larger graphene sheets. Since the nanocrystallite density is controlled by the electron irradiation energy, GSEC film with higher magnetization can be obtained in the future studies, and we can see the possibility of developing GSEC film for magnetic and spintronics applications.

The authors thank the National Nature Science Foundation of China under Grant No. 90923027. The authors also would like to thank Professor X. Liu for experimental support.

[1]T. L. Makarova, B. Sundqvist, R. Hohne, P. Esquinazi, Y. Kopelevich, P. Scharff, V. A. Davydov, L. S. Kashevarova, and A. V. Rakhmanina, Nature **413**, 716 (2001).
[2]A. V. Rode, E. G. Gamaly, A. G. Christy, J. G. Fitz Gerald, S. T. Hyde, R. G. Elliman, B. L. Davies, A. I. Veinger, J. Androulakis, and J. Giapintzakis, Phys. Rev. B **70**, 054407 (2004).
[3]S. Ma, J. H. Xia, V. V. S. S. Srikanth, X. Sun, T. Staedler, X. Jiang, F. Yang, and Z. D. Zhang, Appl. Phys. Lett. **95**, 263105 (2009).
[4]H. S. S. Ramakrishna Matte, K. S. Subrahmanyam, and C. N. R. Rao, J. Phys. Chem. C **113**, 9982 (2009).
[5]P. Esquinazi, D. Spemann, R. Hohne, A. Setzer, K. H. Han, and T. Butz, Phys. Rev. Lett. **91**, 227201 (2003).
[6]S. Talapatra, P. G. Ganesan, T. Kim, R. Vajtai, M. Huang, M. Shima, G. Ramanath, D. Srivastava, S. C. Deevi, and P. M. Ajayan, Phys. Rev. Lett. **95**, 097201 (2005).
[7]M. Wu, E.-Z. Liu, and J. Z. Jiang, Appl. Phys. Lett. **93**, 082504 (2008).
[8]Y. Wang, Y. Huang, Y. Song, X. Zhang, Y. Ma, J. Liang, and Y. Chen, Nano Lett. **9**, 220 (2009).
[9]R. McIntosh, M. A. Mamo, B. Jamieson, S. Roy, and S. Bhattacharyya, Europhys. Lett. **97**, 38001 (2012).
[10]A. Ney, P. Papakonstantinou, A. Kumar, N. G. Shang, and N. Peng, Appl. Phys. Lett. **99**, 102504 (2011).
[11]Y. Zhou, Z. Wang, P. Yang, and F. Gao, J. Phys. Chem. C **116**, 7581 (2012).
[12]J. Zhou, M. M. Wu, X. Zhou, and Q. Sun, Appl. Phys. Lett. **95**, 103108 (2009).
[13]L. Xie, X. Wang, J. Lu, Z. Ni, and Z. Luo, Appl. Phys. Lett. **98**, 193113 (2011).
[14]C. Wang, D. Diao, X. Fan, and C. Chen, Appl. Phys. Lett. **100**, 231909 (2012).
[15]A. C. Ferrari, J. C. Meyer, V. Scardaci, C. Casiraghi, M. Lazzeri, F. Mauri, S. Piscanec, D. Jiang, K. S. Novoselov, S. Roth, and A. K. Geim, Phys. Rev. Lett. **97**, 187401 (2006).
[16]D. Graf, F. Molitor, K. Ensslin, C. Stampfer, A. Jungen, C. Hierold, and L. Wirtz, Nano Lett. **7**, 238 (2007).
[17]A. C. Ferrari and J. Robertson, Phys. Rev. B **61**, 14095 (2000).
[18]S. D. M. Brown, A. Jorio, P. Corio, M. S. Dresselhaus, G. Dresselhaus, R. Saito, and K. Kneipp, Phys. Rev. B **63**, 155414 (2001).
[19]J. Schwan, S. Ulrich, V. Batori, H. Ehrhardt, and S. R. P. Silva, J. Appl. Phys. **80**, 440 (1996).
[20]J. Robertson, Mater. Sci. Eng. R **37**, 129 (2002).
[21]R. Saito, M. Hofmann, G. Dresselhaus, A. Jorio, and M. S. Dresselhaus, Adv. Phys. **60**, 413 (2011).
[22]J. Lee, J. C. Grossman, and M. S. Dresselhaus, Appl. Phys. Lett. **97**, 133102 (2010).
[23]M. Kan, J. Zhou, Y. Li, and Q. Sun, Appl. Phys. Lett. **100**, 173106 (2012).
[24]Y. Ominato and M. Koshino, Phys. Rev. B **85**, 165454 (2012).
[25]H. Santos, A. Ayuela, L. Chico, and E. Artacho, Phys. Rev. B **85**, 245430 (2012).
[26]N. Park, M. Yoon, S. Berber, J. Ihm, E. Osawa, and D. Tomanek, Phys. Rev. Lett. **91**, 273204 (2003).

Downloaded 27 Mar 2013 to 117.32.153.158. This article is copyrighted as indicated in the abstract. Reuse of AIP content is subject to the terms at: http://apl.aip.org/about/rights_and_permissions